

Intensification of Chemically Assisted Melt-Water Explosive Interactions

Anthony A. Sansone

School of Nuclear Engineering
Purdue University
West Lafayette, IN 47907
asansone@purdue.edu

Rusi P. Taleyarkhan

School of Nuclear Engineering
Purdue University
West Lafayette, IN 47907
rusi@purdue.edu

ABSTRACT

A vapor explosion (VE) is a thermo-fluid interaction phenomena in which a hot liquid (e.g. molten metal) transfers its thermal (and possibly also chemical) energy to a cold vaporizing liquid (e.g. water) over an explosive time scale. Significant enhancements are possible by coupling the exothermic oxidation reaction between the molten metal (e.g. Al, Li, Mg) and water with the explosive fragmentation produced by a VE. This paper investigates avenues for controlled initiation and augmentation of the mechanical and thermal energetic output of shock-triggered VEs with Al-GaInSn alloys as a means for impulsive hydrogen generation. Using a submerged electronic bridgewire detonator or rifle primer caps as the shock trigger, experiments were conducted with 10 g single melt drops at an initial temperature of 930-1100 K, aluminum mass contents ranging between 0.3-20 w/o, and water temperatures between 293-313 K. It was found that combined thermal-chemical Al-GaInSn-H₂O explosive interactions could readily be induced and are of greater intensity than the pure thermally driven explosions observed with unalloyed Sn and GaInSn. Shock pressures up to 5 MPa were recorded about 10 cm from the explosion zone; a factor of five higher than the ~1 MPa over pressures generated from spontaneous GaInSn-H₂O explosions. Al-GaInSn-H₂O explosive interactions also exhibited rapid enhancements to the “impulse” H₂ production rate. Hydrogen/vapor bubble volumes up to 460 ml were observed approximately 4 ms after the explosion, equating to a mechanical work and instantaneous power output of 47 J and 11.75 kW respectively. In contrast, the mechanical work output generated by discharging 150 J through the electronic bridgewire was measured to be 16 J, a factor of three lower than the Al-GaInSn-H₂O explosive interaction. Comparisons to relevant experiments of others are made to emphasize the potential advantages of using Al-GaInSn alloys over their pure Al metal counterpart.

KEYWORDS

Vapor explosion, hydrogen, aluminum

1. INTRODUCTION

A vapor (a.k.a. steam) explosion is a thermo-fluid interaction involving intense intermixing and rapid thermal energy transfer between a molten metal and liquid water in an inertially constrained system over

an explosive time scale. The volumetric expansion associated with rapid vaporization of the cold fluid generates pressure waves characteristic of shock traces, followed by the extensive viscous breakup of the hot fluid. The rapidity and violent nature of the interaction mimics the occurrence of an explosion within the hot fluid; hence, the name of the interaction. The potential energetic release accompanying one of these interactions can carry potentially disastrous consequences, and as such, research towards development of a comprehensive understanding of the governing physical mechanisms is of paramount importance for the at-risk industries. These include, most notably, the nuclear industry and the infamous Chernobyl accident, aluminum, magnesium, and steel metals casting industry, liquid natural gas industry, and paper (smelt) casting industry [1-6].

Significant progress has been made over the past several decades to explain these events mechanistically, at a laboratory scale with gram to kilogram melt quantities, thereby identifying pathways with which these explosions may be prevented. Dullforce et al. investigated molten tin-water interactions to develop the concept of a so-called thermal interaction zone (TIZ), within which spontaneous explosions occur [7]. Board and Hall demonstrated the principle of intentionally inducing (triggering) explosions by exposing the submerged molten mass to a forceful mechanical disturbance [8], whereby the velocity induced in the water at the shock pressure front drives the liquid-vapor interface into contact with the melt. Schins [9] has documented the characteristic pressure signatures of the devices most commonly employed in external triggering-related experiments: detonators, exploding bridgewires, and mechanical impactors. Comprehensive reviews on the theoretical and experimental work pertaining to spontaneous and triggered explosions have been compiled by Fletcher et al. [10,11] and Corradini [12].

In the instances where a chemical reaction between the water vapor and molten melt (e.g., Al, Li, Zr) is thermodynamically favorable, the rapid surface area enhancement from fragmentation may serve as a mechanical “catalyst”, creating the opportunity for positive feedback with the exothermic oxidation reaction. Several cases of energetic, actively triggered, thermal-chemical explosions have been observed in aluminum-water systems [13-15]. These interactions are extremely violent, and often accompanied with extremely bright emissions of light and explosive production of large quantities of hydrogen gas as a result of achieving chemical ignition. These ignition-type explosions have, however, conventionally required impractically high (>1500 K) initial melt temperatures. At these temperatures the self-heating from the exothermic oxidation reaction slows the rate at which oxide crystals nucleate at the reaction front, which subsequently delays the formation of a cohesive oxide surface layer and enables the reaction to continue [16].

In the past we reported on studies to evaluate spontaneous melt-water explosion phenomena using Sn, GaInSn (a eutectic alloy of 65 w/o Ga, 25 w/o In, and 15 w/o Sn with a melting point of 254 K), and various alloys of Al-GaInSn. GaInSn possesses the novel ability to disrupt the cohesiveness of the aluminum surface oxide layer, allowing for sustained oxidation and hydrogen production at room temperature [17]. However, the production of a noncondensable gas (NCG) also acts to quench the explosive event by stabilizing the melt-water interface, as we have reported earlier [18]; unless another competing mechanism can be introduced. One such competing approach involves the use of an external shock pulse, which can overcome the stabilizing effect of NCGs, and yet, allow rapid fragmentation simultaneously with “impulsive” hydrogen production at modest superheats. Thus, it was hypothesized that it may be possible to achieve energetic vapor explosion-driven aluminum-water combustion at modest (~200 K versus ~600 K) superheats. This paper reports on the findings from these studies.

2. EXPERIMENTAL SYSTEM AND TEST MATRIX

Figure 1 contains a schematic of the experimental test system. The system consists of a cylindrical 700 W radiant heater enclosed by thick blocks of calcium silicate thermal insulation. During heating and up unto the moment prior to melt discharge, metal samples were located within a high purity machineable alumina-bisque crucible. To minimize chemical attack during heating, the crucible and plunger were

coated with a boron-nitride aerosol spray before each experiment. To further prevent melt oxidation during heating, argon gas was initially purged directly into the heater for 30 seconds at 240 kPa, after which the oven was brought to the desired temperature, and then the argon gas was fed at 108 kPa for the remainder of the test. Temperature control and melt discharge are handled by a Labview™ virtual instrument and Arduino™ microcontroller. The melt discharge is automated by affixing a strong solenoid (manually activated through the virtual instrument) just above the crucible plunger, which is fitted with a rare earth magnet. The explosion chamber is made of polycarbonate and filled with distilled water. The chamber is open ended and freely exposed to the surrounding air, though our future plans include closed chambers for purposes of gas collection and dynamic pressure monitoring.

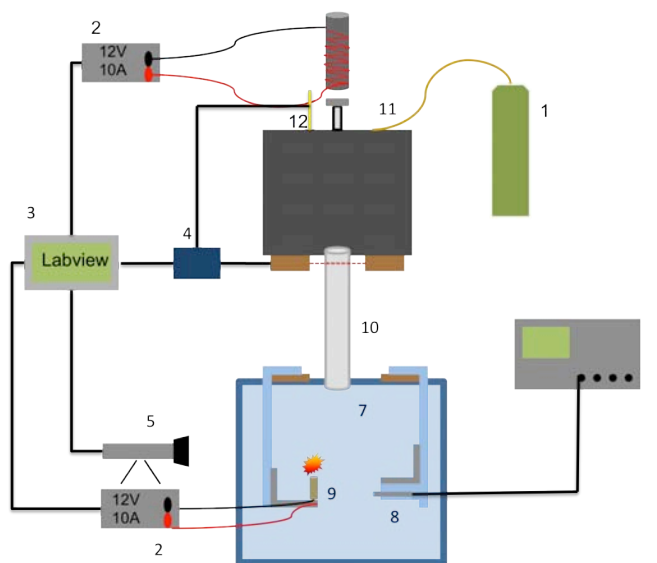


Figure 1. Schematic diagram of the system used for the Sn-H₂O and Al-GaInSn-H₂O melt interaction experiments (1) Argon supply (2) direct current power source (3) PC with Labview™ virtual instrument (4) Arduino™ microcontroller (5) high speed camera (6) digital oscilloscope (7) explosion containment (8) Tourmaline® pressure sensor (9) shock generator (10) atmospheric containment tube (11) heater containment

Part of the current study includes testing of various underwater shockwave generation sources as a means to actively induce explosion triggering; two primary methods were employed. The first method involved discharging (shorting) an ultra low inductance Maxwell™ 3 kV 63 μF capacitor through a thin bridgewire. This technique is commonly referred to as an electrical bridgewire (EBW). The other method involved detonating an electrically activated Remington Model 700 EtronX™ (ETX) large rifle primer using a 200 V 460 μF electrolytic capacitor. Timing of the EBW detonation was accomplished by monitoring the voltage from two collimated, infrared photodetector sets attached right below the crucible discharge hole. The delay between melt discharge and EBW detonation was calibrated such that the melt was within ~3 cm from the EBW in the vertical plane and ~5 cm in the horizontal plane. During the test, an Agilent™ 100 MHz digital storage oscilloscope was triggered to acquire and store pressure pulse data received from a model 138A06 Tourmaline ICP® underwater blast sensor. The pressure sensor was positioned ~6 cm from the EBW and ~10 cm from the targeted location of the melt-water interaction. A high speed digital movie camera from Motion Engineering Corporation, Inc. operated at 500 frames per second, captured the interaction dynamics. For the subset of experiments involving triggered Al-GaInSn-H₂O explosions, select frames from the high-speed video were analyzed to estimate

the volume of H₂ generated immediately following the explosion. Finally, for the subset of experiments involving Sn-H₂O interactions, the debris at the bottom of container was photographed, removed, dried, and sieved for analysis of fragmentation.

The test matrix for this study is shown in Table 1 and was guided from insights we derived from our past reported studies [18]. The chosen metals for this study were Sn, GaInSn, Ga, and an Al-GaInSn alloy. Melt mass sample sizes varied from 10 to 15 grams and melt temperatures ranged from 923-1123 K. Water temperatures ranged from 293-338 K for spontaneous explosion experiments and from 278-313 K for experiments concerning Al-H₂O reactions. Experiments regarding water chemistry manipulation involved NaCl additions of 2.5-10 w/o.

Table I. Experimental Test Matrix

Material	Melt Mass (g)	Melt Temp (K)	NaCl Content (%)	External Trigger
Sn	10-15	923-1073	2.5-10	ETX, EBW
GaInSn	10-15	923-1073	N/A	ETX, EBW
Ga	10	1123	10	N/A
Al-GaInSn	10	800-850	2.5-10	ETX, EBW

3. EXPERIMENTAL RESULTS AND FINDINGS

The set of experiments conducted in this study constituted a natural advancement of the baseline spontaneous explosion experiments reported by Zielinski et al [18]. Several important conclusions were drawn from our past study and will be briefly summarized as they strongly helped shape our test matrix. First, the amount of fragmentation from spontaneous explosive interactions in Sn-H₂O and GaInSn-H₂O systems was semi-quantitatively categorized as very good (VG), good (G), some (S), and none (N). The extent of fragmentation from GaInSn interactions was much greater than Sn-H₂O interactions. VG type explosions were identified by interactions in which < ~60% of the solidified debris was over 2 mm, G type interactions were those in which < ~70% of the debris was over 2 mm, while the S and N interactions involved < ~95%. The second main finding was that adding as little as 0.3 percent by weight of Al to GaInSn conclusively suppressed spontaneous explosions at all thermal combinations, indicating the overwhelming influence non-condensable gases have on arresting film collapse. Finally, it was found that gallium, like aluminum, failed to explode spontaneously at thermal conditions inside the TIZ. However, the addition of 10 w/o aqueous NaCl generated VG type explosive interactions.

3.1. Initiation of Melt-Water Interactions via Passive Environment Manipulation

The explosive transformation seen with the molten Ga interactions in aqueous NaCl spawned attempts to induce similar transformations in the Al-GaInSn system. The Al-GaInSn alloy remained familiarly non-explosive at the nominal test conditions of 293-313 K water temperature and 1073-1123 K melt temperature. Spontaneous explosive interactions were however observed for only one particular set of conditions. Specifically, for the case of 278 K water temperature and approximately 5 w/o NaCl, explosions were attained with semi-good reproducibility. The fragments visible in Fig. 1 indicate a G to VG type interaction for allows containing 0.3 and 4.5 w/o Al, respectively. It can be seen that, though a spontaneous explosion did occur with the 5 w/o Al-GaInSn alloy, the extent of the fragmentation does not

resemble that which is expected for a pure GaInSn-H₂O interaction at the same thermal conditions. This suggests that the additional H₂ produced by the higher aluminum content was negatively impacting film collapse.



Figure 2. Fragmentation results from VG and G type spontaneous explosions in 10 w/o aqueous NaCl with 0.3 w/o (top) and 5 w/o (bottom) Al-GaInSn alloys respectively

The already documented [18] behavior of Sn and the ability to quantitatively characterize the explosion intensity through fragment sieving made Sn an ideal choice to gain further insight into the effects of NaCl on explosion triggerability. Test cases were run at variable NaCl concentrations ranging between 2.5 and 10 w/o. Similar to the scoping studies with Ga, the presence of NaCl had the effect of accelerating explosion onset following initial contact with the water surface. While explosions for the lower NaCl concentration of 2.5 w/o occurred at a depth slightly below the surface (yet still above the triggering depth for the baseline 0 w/o case), for concentrations of 5 w/o, onset occurred in the immediate vicinity of the air-water interface.

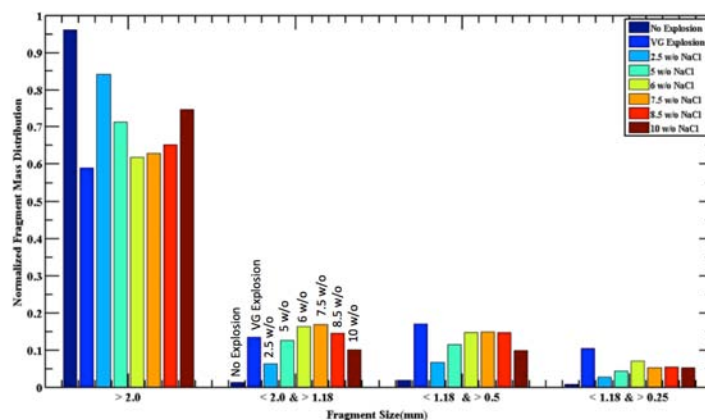


Figure 3. Normalized mass distribution of Sn comparing degree of fragmentation at various NaCl contents

Analysis of the fragment mass distribution revealed that the intensity of the Sn interaction does not scale proportionately with the enhancement in triggering ability. The mass distributions for the various NaCl concentrations are shown in Fig. 3. Based on data analysis the optimal NaCl concentration to maximize fragmentation appears to be in the vicinity of ~ 6 w/o. Interestingly, even the most energetic interaction did not surpass the amount of fragmentation produced by the baseline spontaneous VG explosion case.

3.2. Initiation of Melt-Water Interactions via External Shock Triggers

Experiments were next conducted to assess the capability for on-demand externally triggered initiation of explosive interactions for nominally inert thermal and melt combinations. These experiments, using Sn as the host melt, involved comparing the ensuing melt-water explosion intensity to its spontaneous explosion counterpart. The melt and water temperatures were set as 923 K and 293 K respectively and the drop height increased from its nominal distance of 20 cm to 40 cm. Note that this thermal (melt and water temperature) combination actually lies within the TIZ, implying that explosions should occur spontaneously. However, by increasing the drop height, additional gases are entrained into the interfacial vapor layer, inhibiting spontaneous film collapse. Thus, the observance of any explosions is a direct attributed consequence of the external shock trigger.



Figure 4. Fragmentation of Sn melts exposed to variable amplitude shock pulses from detonation of a submerged electrical bridgewire. The left and right photos correspond to capacitor energies of 25 J and 32 J respectively.



Figure 5. Sn fragmentation shock-triggered using an EtronX™ electronic rifle primer

Figure 4 depicts the transition from purely quenching (viz. an N type interaction) to complete catastrophic, explosive fragmentation induced by the EBW detonator using capacitor discharge energies of 25 J versus 32 J. Significant improvements in the degree of fragmentation, as compared to the VG case depicted in Fig. 2 from Zielinski et al., are evident through visual inspection alone. Shock-triggered explosion amplification was also observed when using the EtronX™ rifle primer as the trigger source. The EtronX™ primer initiated the most violent Sn-H₂O explosion recorded to date. The resultant fragmentation, seen in Fig. 5, shows a visually distinct margin of improvement over the already enhance EBW case.

Quantifiable comparisons of the fragment mass distribution for each triggering technique are presented in Fig. 6. Shock-amplified explosions showed 40% improvements over the baseline VG grade interaction for the coarsest size bin, converting over 80% of the original 10 g mass to sub-millimeter scale particulates. Equally impressive is the conversion of over 50% of the original melt mass to 10² micron-scale powders. Quantitative mass distribution data was not possible below 250 μm (due to the sieving system available for these studies).

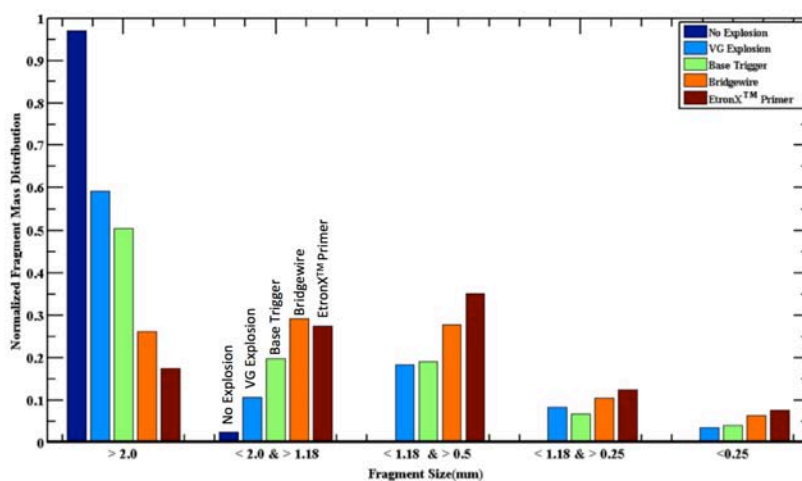


Figure 6. Comparison of the fragment mass distributions generated using various external triggering techniques

3.3 Vapor Explosion Driven Combustion Using Molten Al-GaInSn Alloys in Water

Using the EBW shock triggering method reported earlier, we have shown that combined thermal-chemical-explosive interactions can be reliably induced in Al-GaInSn-H₂O systems at various parametric configurations. These include aluminum mass contents ranging between 0.3 and 20 w/o and water temperatures ranging from 293-313 K. These combined thermal-chemical explosions appear to be of significantly greater intensity than the pure thermally driven explosions observed with Sn and GaInSn. Evidence of enhanced H₂ production from vapor explosion facilitated aluminum-water combustion was observed both immediately following the explosion (i.e. within 10 ms), as well as several hundred milliseconds after fragment quenching.

3.3.1 Impulse Hydrogen Production

Analysis of the high-speed (500 fps) images reveals Al-GaInSn-H₂O explosions generate a large hydrogen/vapor bubble, which lasts on the order of ten milliseconds. This bubble appears to be

completely cohesive, which differs from those reported earlier with purely thermal explosions with Sn and GaInSn [18], which may be more appropriately interpreted as a fine particulate-vapor cloud. The temporal evolution of the hydrogen/vapor bubble from a typical 20 w/o Al-GaInSn explosion is shown in Fig. 7.

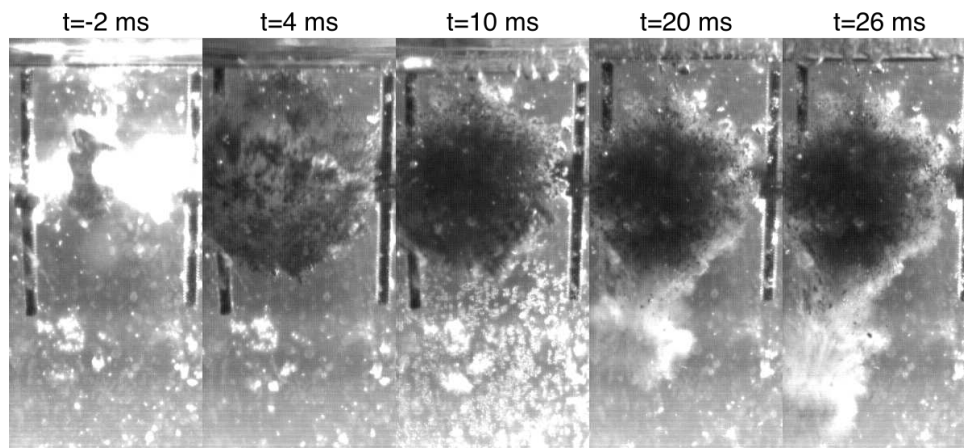


Figure 7. High speed images showing the time evolution of the hydrogen/vapor bubble produced by a lower superheat (~150 K) 20 w/o Al-GaInSn-H₂O explosion

The first frame on the left in Fig. 7, corresponding to a time of milliseconds before the Al-GaInSn explosion, shows the remnants of the bright flash emitted by the EBW detonation. Four milliseconds after the explosion the hydrogen bubble has grown to its maximum diameter. At a time of ten milliseconds the bubble has collapsed. The water hammer from the imploding bubble causes additional melt-water mixing and induces a second explosion, as evidenced by the numerous cavitation bubbles seen in the bottom right portion of the image. At a time of 20 milliseconds the high pressures generated by the second interaction have ejected a portion of the melt mass outward from the bubble center. Finally, twenty-six milliseconds after the explosion, the ejected mass has almost entirely left the camera window and the melt fragments have begun their free-fall descent through the water containment.

Following the initial burst, a sustained increase in the hydrogen volumetric production rate is seen over instances where an explosion did not occur. Fragmentation of the melt serves to not only increase the reaction surface area, but also reduces the distance the Al must diffuse to reach the reaction front (i.e. the surface of the fragment). Since the current explosion containment is an open system, quantitative temporal monitoring of H₂ generation is not possible. However, for qualitative purposes the upper collage of images in Fig. 8 gives a visual illustration of the hydrogen generated two hundred and four hundred milliseconds after a 10 w/o Al-GaInSn explosive interaction, while the lower collage of images depicts the hydrogen generated by a 10 w/o Al-GaInSn alloy undergoing pure quenching. At time equals four hundred milliseconds the quenched Al-GaInSn alloy has almost fallen outside the camera window and has just begun to produce small quantities of hydrogen. In comparison, the Al-GaInSn alloy which underwent an explosive interaction produced an opaque cloud of hydrogen bubbles which encompasses almost the entire camera window.

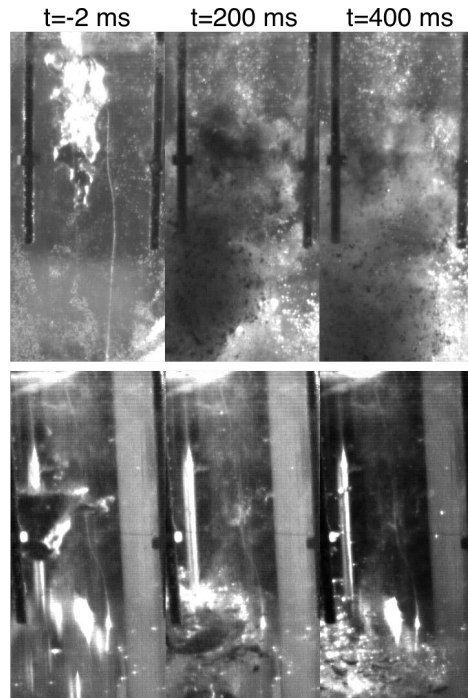


Figure 8. High-speed images depicting the sustained enhancement in the hydrogen production rate by a 10 w/o Al-GaInSn melt alloy for the cases of an explosive interaction (top) and non-explosive slow quenching (bottom)

3.3.2 Shock Signals and Expansion Work

Figure 9 shows the pressure time history of the shocks generated from detonation of the EBW trigger (left) and the resulting combined thermal-chemical explosion with a 20 w/o Al-GaInSn alloy (right). For this set of experiments the energy discharged through the bridgewire was 150 J. The EBW is seen to generate shock transients with an amplitude of ~ 9 MPa and a pulse width of $10 \mu\text{s}$. The shock trace from the Al-GaInSn- H_2O explosion generated pressures of ~ 5 MPa with a pulse width of $\sim 20 \mu\text{s}$, which is a factor of five higher than the ~ 1 MPa over-pressures generated from spontaneous and triggered GaInSn- H_2O interactions.

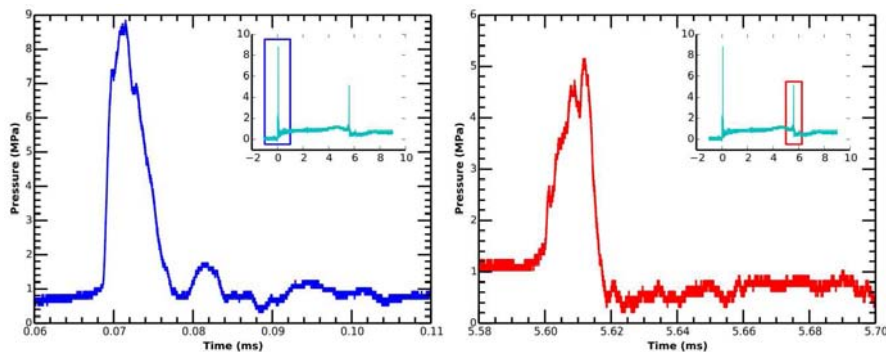


Figure 9. Pressure time history of the shocks generated from the EBW trigger (left) and the thermal-chemical explosion between a 20 w/o Al-GaInSn alloy and water (right). The entire pressure trace, as seen from the oscilloscope, is shown in the upper right corner.

Figure 10 gives a side by side comparison of the maximum bubble diameters produced from detonation of the EBW trigger (left) and the resulting combined thermal-chemical explosion with a 20 w/o Al-GaInSn alloy (right); the same experiment which yielded the shock pressures shown in Fig. 9. By assuming both bubbles to be circular, a simple PdV analysis can be conducted to compare the expansion work output of the EBW and thermal-chemical explosion. The bubble volume formed from the Al-GaInSn-H₂O interaction was estimated to be approximately 459 ml, a factor of three higher than the bubble generated by the EBW detonation, which had an estimated volume of approximately 146 ml. These volumes correspond to a work output of 47 J and 16 J, respectively. The hydrogen bubble grew to its maximum observed diameter within four milliseconds, which equates to an instantaneous mechanical power of 11.75 kW.

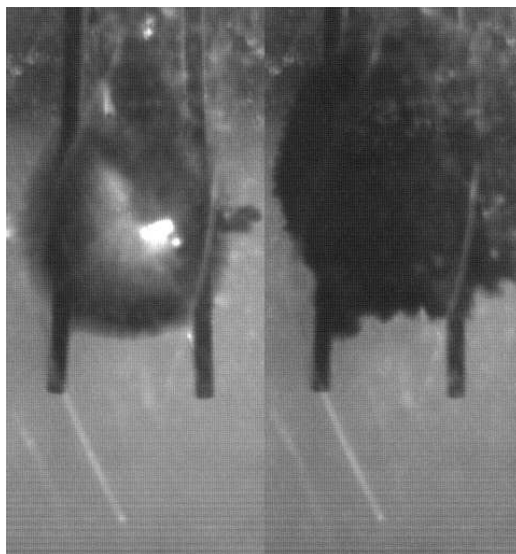


Figure 10. Comparison of the explosion bubble produced using 150 J to detonate an EBW (left) and a 20 w/o Al-GaInSn-H₂O vapor explosion (right)

4. DISCUSSION

One of the major initiatives of this work was to assess the capability of Al-GaInSn alloys to produce hydrogen on an explosive timescale. In contrast to pure aluminum or other standard aluminum alloys, Al-GaInSn alloys do not form a cohesive surface oxide layer. Without this diffusion barrier the aluminum can continually react with water at room temperature to near theoretical maximum yields. Thus, in order to estimate the reaction efficiency, it is of interest to this work to distinguish the hydrogen generated immediately (within milliseconds) following the explosion versus that generated (over minutes to hours) after quenching.

4.1 Chemical Reaction Efficiency

Assuming the contribution from water vapor to the bubble volume can be neglected, we can approximate the mass of hydrogen, which was generated during the initial explosive burst shown in Fig. 10, using the ideal gas law equation of state. Since the bubble volume was analyzed at its maximum diameter, corresponding to the inflection point of the expansion work output, the internal pressure and pressure of the bubble were assumed to be equal to the ambient temperature and pressure; this provides an upper bound on the quantity of hydrogen within the bubble. Using these assumptions. The mass of H₂ was

estimated to be approximately 17% of the theoretical maximum mass set by the two grams of aluminum initially present in the melt alloy.

It should also be realized that the melt isn't a pure mass of aluminum. Rather, it is an alloy composed of twenty percent aluminum by mass. An upper bound on the impulse burst reaction efficiency can be set by assuming that the drop breakup (fragmentation) is a single step process and that the breakup time is much less than the diffusion time. Experimental measurements of the diffusion coefficient of Al in GaInSn are not available. Bräuer et al. [19] has reported the diffusional coefficient of Al in molten Ga to be 1073 K to be $1.36 \cdot 10^{-4} \text{ cm}^2/\text{s}$. Using this value, the maximum distance Al could diffuse in the four millisecond window following the explosion is 15 μm . Using the mass distribution from triggered explosions with Sn shown in Fig. 6, it can be seen that greater than 90% of the fragments have diameters larger than 250 μm . Thus, the assumption of neglecting diffusional effects has merit. Finally, assuming a homogenous distribution of aluminum, the maximum concentration of aluminum at the fragment surface immediately following the explosion can only be twenty percent of the initial two grams. Under these assumptions, the 17% absolute reaction efficiency translates to as high as 85% for the impulse reaction efficiency.

4.2 Comparison to Nelson's Single Drop, High Superheat, Triggered Aluminum Experiments

A literature search revealed that data on combined thermal-chemical explosions with gram scale aluminum alloys is very limited. Past experiments have predominantly been conducted with 10 Kg quantities of aluminum [2, 20]. However, at the 10^3 kilogram scale the temperature threshold for an ignition type explosion decreases to just above the melting temperature of aluminum, making any comparison to the work presented here irrelevant. The closest analogue to our experiments was conducted by Nelson [13] and involved triggered explosions of 1-10 g drops of pure Al and the Al-6061 alloy at initial melt temperatures ranging between ~ 1200 - 1800 K.

Table 2 contains comparisons between the interaction with the 20 w/o Al-GaInSn alloy (shown in Fig. 9 and Fig. 10) with the interactions from two explosions using pure aluminum, as reported by Nelson [13]. The Al-GaInSn alloys significantly outperform their pure Al counterpart, generating a factor of 18x and 4x more hydrogen on a per gram basis, despite the 200 K and 400 K respective reduced initial melt temperature.

Table 2 Comparison between explosions induced by a shock trigger with the Al-GaInSn alloy and pure Al, as reported by Nelson [13]

Melt Alloy	Nelson [13]		This Paper
	Al	Al-6061	20 w/o Al-GaInSn
T_{melt} (K)	1243	1468	1073
Al Mass (g)	6.54	4.50	2.02
V_{H_2} (cm ³)	82	267	459
$V_{\text{H}_2}/m_{\text{Al}}$ (cm ³ /g)	12.3	59.4	226.7
Efficiency	0.8	3.8	17.1

5. CONCLUSIONS

This paper has presented results and analyses of vapor explosion studies with melt masses of Sn, Ga, GaInSn, and Al-GaInSn alloys dropped into water with various means for initiating or amplifying an explosive melt-water interaction. The effect of aqueous NaCl on explosion triggering and intensity was investigated as a passive technique for triggering an explosive reaction for an otherwise inert system. Al-GaInSn alloys remained explosively inert at nominal test conditions, yet interestingly exploded spontaneously at the combination of 278 K water temperature and 5 w/o NaCl. Quantitative assessments of spontaneous explosions were conducted in the Sn-NaCl system, indicating that the presence of NaCl enhances the likelihood of spontaneous triggering but at the expense of explosion intensity.

As an alternative to passive manipulation for the onset of explosive events, our studies have revealed that such explosions can be controllably initiated by shocks generated from an EBW as well as novel EtronXTM electronic rifle primers. Shock amplified explosions showed 40% improvements over the baseline VG grade interaction for the coarsest size bin, converting over 80% of the original mass to sub-millimeter scale particulates.

Combined chemical and thermal interaction-based VEs were reliably induced via shock-triggering in Al-GaInSn-H₂O systems at various Al mass contents and water temperatures. Data collected using high-speed imaging and piezoelectric pressure transducers indicate Al-GaInSn-H₂O triggered explosive interactions are of greater intensity than with pure GaInSn, highlighting the dominant contribution of the added chemical component to the energetic output. Experiments conducted with 20 w/o Al-GaInSn alloys generated hydrogen/vapor explosion bubble volumes as large as ~460 ml; a notable factor of three larger than the explosion bubble volume produced by discharging 150 J into the EBW trigger. In comparison with available, analogous, triggered-explosion studies with Al melts [13], Al-GaInSn alloys generated more hydrogen per gram of aluminum.

It is worth noting that these findings were obtained with relatively low aluminum content alloys. By increasing the alloy's aluminum mass fraction, additional gains in the instantaneous power output may be possible as a result of the additional aluminum present at the reaction surface immediately following the explosion; though, additional studies are needed to understand this parametric relationship in detail.

ACKNOWLEDGMENTS

This research was sponsored by the State of Indiana, Purdue University and funding support from Sagamore Adams Laboratories, LLC. The cooperation and assistance from Purdue University's Metastable Fluid Research Laboratory and especially past work of Steven Zielinski and Matthew Ziolkowski are highly appreciated. Advice and Assistance from Dr. Clifford Bedford of the U.S. Department of Defense's Office of Naval Research is gratefully acknowledged. Assistance from Purdue University's REM department is similarly appreciated.

REFERENCES

1. Rasmussen, N., 1975. Reactor Safety Study: An Assessment of Accident Risks in U.S. Commercial Nuclear Power Plants. Tech. Rep. WASH-1400(NUREG-75/014), U.S. Nuclear Regulatory Commission.
2. Taleyarkhan, R., 2005. "Vapor Explosion Studies for Nuclear and Non-Nuclear Industries". *Nuclear Engineering and Design*, 235(10-12), pp. 1061-1077.
3. Epstein, S., 2005. "A Summary of Findings from Twenty Years of Molten Metal Incident Reporting". In *Light Metals 2005*, H. Kvande, ed. The Minerals Metals and Materials Society.

4. Alfadala, H., Reklaitis, G., and El-Halwagi, M., 2009. "Nuclear Technology for Frontier Advances in the Natural Gas Industry". In Proceedings of the 1st Annual Gas Processing Symposium, H. Alfadala, G. Reklaitis, and M. El-Halwagi, eds., *Advances in Gas Processing*, Elsevier Science, pp. 162 – 170.
5. Reid, R., 1983. "Rapid Phase Transitions from Liquid to Vapor". Vol. 12 of *Advances in Chemical Engineering*. Academic Press, pp. 105 – 208.
6. Shick, P. E., and Grace, T. M., 1982. *Review of Smelt-Water Explosions*. Institute of Paper Chemistry.
7. Dullforce, T., Buchanan, D. J., and Peckover, R. S., 1976. "Self-Triggering of Small-Scale Fuel-Coolant Interactions: I. Experiments". *Journal of Physics D: Applied Physics*, 9(9), p. 1295.
8. Board, S., and Hall, R., 1975. "Thermal Explosions at Molten Tin/Water Interfaces". *Moving Boundary Problems in Heat Flow and Diffusion*, pp. 259–269.
9. Schins, H., 1986. "Characterization of Shock Triggers used in Thermal Detonation Experiments". *Nuclear Engineering and Design*, 94(1), pp. 93 – 98.
10. Fletcher, D., 1995. "Steam Explosion Triggering: A Review of Theoretical and Experimental Investigations". *Nuclear Engineering and Design*, 155(1-2), pp. 27 – 36.
11. Fletcher, D., and Theofanous, T., 1997. "Heat transfer and Fluid Dynamic Aspects of Explosive Melt–Water Interactions". *Advances in Heat Transfer*, 29, pp. 129– 213.
12. Corradini, M., Kim, B., and Oh, M., 1988. "Vapor Explosions in Light Water Reactors: A Review of Theory and Modeling". *Progress in Nuclear Energy*, 22(1), pp. 1 – 117.
13. Nelson, L., 1995. "Steam Explosions of Single Drops of Pure and Alloyed molten aluminum". *Nuclear Engineering and Design*, 155(1-2), pp. 413–425.
14. Theofanous, T. G., Chen, X., Di Piazza, P., Epstein, M., and Fauske, H. K., 1994. "Ignition of Aluminum Droplets Behind Shock Waves in Water". *Physics of Fluids*, 6(11), pp. 3513–3515.
15. Cho, D., Armstrong, D., and Anderson, R., 1995. "Combined Vapor and Chemical Explosions of Metals and Water". *Nuclear Engineering and Design*, 155(1- 2), pp. 405 – 412.
16. Epstein, M., Fauske, H., and Theofanous, T., 2000. "On the Mechanism of Aluminum Ignition in Steam Explosions". *Nuclear Engineering and Design*, 201(1), pp. 71 – 82.
17. Ziebarth, J.T., Woodall, J.M., Kramer, R.A., and Choi, G., 2011. "Liquid Phase-Enabled Reaction of Al-Ga and Al-Ga-In-Sn Alloys with Water". *International Journal of Hydrogen Energy*, 36(9), pp. 5271 – 5279.
18. Zielinski, S. M., Sansone, A. A., Ziolkowski, M., and Taleyarkhan, R. P., 2011. "Prevention and Intensification of Melt-Water Explosive Interactions". *Journal of Heat Transfer*, 133(7), p. 071201.
19. Bräuer, P., and Müller-Vogt, G., 1998. "Measurements of Aluminum Diffusion in Molten Gallium and Indium". *Journal of Crystal Growth*, 186(4), pp. 520–527.
20. Long, G., 1957. "Explosions of Molten Aluminum in Water-Cause and Prevention". *Metal Progress*, 71(5), pp. 107–112.